Physics Letters B 793 (2019) 200–205

Contents lists available at ScienceDirect

Physics Letters B

www.elsevier.com/locate/physletb

Imaginary potential of heavy quarkonia from AdS/QCD

Zi-qiang Zhang [a,*], Xiangrong Zhu [b]

[a] School of Mathematics and Physics, China University of Geosciences, Wuhan 430074, China
[b] School of Science, Huzhou University, Huzhou 313000, China

ARTICLE INFO

Article history:
Received 4 January 2019
Received in revised form 18 April 2019
Accepted 24 April 2019
Available online 26 April 2019
Editor: J.-P. Blaizot

ABSTRACT

The imaginary part of a heavy quarkonium potential is studied at finite temperature and chemical potential using a holographic AdS/QCD model with conformal invariance broken by a background dilaton. It is shown that the presence of the confining scale increases the absolute value of the imaginary potential thus increasing the thermal width, reverse to the effect of the chemical potential. One step further, the results imply that the inclusion of the confining scale reduces the quarkonia dissociation while the chemical potential enhances it.

1. Introduction

It is by now well accepted that the heavy ion collisions at RHIC and LHC have produced a new state of matter so-called quark gluon plasma (QGP) [1]. One of the main experimental signatures of the QGP formation is melting of heavy quarkonia. It was argued [2] earlier that in a thermal bath, the binding interaction of the heavy quark-antiquark ($Q\bar{Q}$) pair is screened by the medium, resulting in the quarkonia dissociation. But recently some research suggests that the imaginary part of the potential, $\mathrm{Im}V_{Q\bar{Q}}$, may be a more important reason than screening [3–8]. Moreover, this quantity can be used to estimate the thermal width. In perturbative QCD, $\mathrm{Im}V_{Q\bar{Q}}$ has been studied in many papers, see e.g. [9–11]. However, numerous experiments indicate that QGP is strongly coupled [12]. Thus, calculational tools for strongly coupled, real-time QCD dynamics are needed. Such tools are now available via the AdS/CFT duality.

AdS/CFT [13–15], the duality between the type IIB superstring theory formulated on $\mathrm{AdS}_5 \times S^5$ and $\mathcal{N}=4$ supersymmetric Yang-Mills theory (SYM) in four dimensions, has yielded many important insights for studying different aspects of QGP (see [16] for a good review). In this approach, Noronha and Dumitru have studied the $\mathrm{Im}V_{Q\bar{Q}}$ for $\mathcal{N}=4$ SYM theory in their seminal work in [17]. Therein, the $\mathrm{Im}V_{Q\bar{Q}}$ is related to the effect of thermal fluctuations due to the interactions between the heavy quarks and the medium. Later, this idea has been extended to various cases. For example, the $\mathrm{Im}V_{Q\bar{Q}}$ of static quarkonia is studied in [18,19]. The $\mathrm{Im}V_{Q\bar{Q}}$ of moving quarkonia is investigated in [20,21]. The effect of the medium on the $\mathrm{Im}V_{Q\bar{Q}}$ of moving quarkonia is analyzed in [22]. The finite 't Hooft coupling corrections on $\mathrm{Im}V_{Q\bar{Q}}$ is addressed in [23]. Also, this quantity has been discussed in some AdS/QCD models [24,25]. Besides, there are other ways to study $\mathrm{Im}V_{Q\bar{Q}}$ from holography [26–28].

Here we give such analysis in a soft wall-like model with finite temperature and chemical potential, viz. the $\mathrm{SW}_{T,\mu}$ model, which is defined by the AdS-Reissner Nordstrom black-hole (AdS-RN) metric multiplied by a warp factor. Such a model is motivated by the soft wall model of [29] that introduced a quadratic dilaton to emulate confinement in the boundary theory at vanishing temperature. In Ref. [30], it was proposed to study the heavy quark free energy as well as the QCD phase diagram, and the results show that it could provide a nice phenomenological description of quark-antiquark interaction and other hadronic properties. Further studies of models of this type, see [31–34]. Inspired by this, in this paper we investigate the $\mathrm{Im}V_{Q\bar{Q}}$ of heavy quarkonia in $\mathrm{SW}_{T,\mu}$ model. Specifically, we would like to see whether chemical potential and confining scale have the same effect on $\mathrm{Im}V_{Q\bar{Q}}$. Also, this work could be regarded as the generalization of [17] to the case with chemical potential and confining scale.

The rest of the paper is as follows. In the next section, we introduce the $\mathrm{SW}_{T,\mu}$ model given in [30]. In section 3, we evaluate the expressions for the real and imaginary part of the heavy quark potential, in turn. In section 4, we study the effects of chemical potential and confining scale on $\mathrm{Im}V_{Q\bar{Q}}$ and analyze how they affect the thermal width as well as the quarkonia dissociation. The last part is devoted to conclusion and discussion.

* Corresponding author.
E-mail addresses: zhangzq@cug.edu.cn (Z.-q. Zhang), xrongzhu@zjhu.edu.cn (X. Zhu).

https://doi.org/10.1016/j.physletb.2019.04.057

2. Background geometry

Let us begin with the holographic models in terms of the action [35]

$$S=\frac{1}{16\pi G_5}\int d^5x\sqrt{-g}(\mathcal{R}-\frac{1}{2}\partial_M\phi\partial^M\phi-V(\phi) -\frac{f(\phi)}{4}F_{MN}F^{MN}), \tag{1}$$

where G_5 is the five-dimensional Newton constant. g represents the determinant of the metric g_{MN}. $\mathcal{R}$ denotes the Ricci scalar. ϕ refers to the scalar that induces the deformation away from conformality. $V(\phi)$ stands for the potential which contains the cosmological constant term 2Λ and some other terms. $f(\phi)$ and F_{MN} are the gauge kinetic function, the field strength tensor, respectively.

The equations of motion associated with action (1) are

$$\mathcal{R}_{MN}-\frac{1}{2}\mathcal{R}g_{MN}=T_{MN}, \tag{2}$$

$$\nabla_M\Big(f(\phi)F^{MN}\Big)=0, \tag{3}$$

$$\nabla^M\nabla_M\phi=V'(\phi)+\frac{f'(\phi)}{4}F_{MN}F^{MN}, \tag{4}$$

with

$$T_{MN}=\frac{1}{2}[f(\phi)(F_{MA}F^A_N-\frac{1}{4}g_{MN}F_{AB}F^{AB}) +(\partial_M\phi\partial_N\phi-\frac{1}{2}g_{MN}\partial_A\phi\partial^A\phi)-g_{MN}V(\phi)], \tag{5}$$

where ∇_M is the Levi-Civita covariant derivative with respect to g_{MN}.

Note that for vanishing ϕ, the AdS black spacetime arises as a solution of (2)-(5). Furthermore, if one considers a non-vanishing gauge-field component A_0 with the boundary conditions

$$A_0(z=0)=\mu R,\qquad A_0(z_0=z_h)=0, \tag{6}$$

the AdS-RN space-time can be obtained by solving (2)-(5). The corresponding metric is

$$ds^2=\frac{R^2}{z^2}(-f(z)dt^2+d\vec{x}^2+\frac{dz^2}{f(z)}), \tag{7}$$

with

$$f(z)=1-(1+\frac{\mu^2z_h^2}{3})\frac{z^4}{z_h^4}+\frac{\mu^2z_h^2}{3}\frac{z^6}{z_h^6}, \tag{8}$$

where μ is the chemical potential. R is the AdS radius. z is the coordinate describing the 5th dimension with $z=0$ the boundary and $z=z_h$ the horizon.

The gauge-field component reads

$$A_0(z)=\mu R(1-\frac{z^2}{z_h^2}). \tag{9}$$

The temperature reads

$$T=\frac{1}{\pi z_h}(1-\frac{Q^2}{2}), \tag{10}$$

with

$$Q=\mu z_h/\sqrt{3}, \tag{11}$$

where Q is the charge of the black hole and constrained in the range $0\le Q\le\sqrt{2}$.

To emulate confinement in the boundary theory, one can introduce a warp factor $h(z)$ to the metric, similar to the procedure in [29,36]. Then the metric of the $SW_{T,\mu}$ model is [30]

$$ds^2=\frac{R^2}{z^2}h(z)(-f(z)dt^2+d\vec{x}^2+\frac{dz^2}{f(z)}),\qquad h(z)=e^{c^2z^2} \tag{12}$$

where c represents the deformation parameter which has the dimension of energy. Note that we will not focus on a specific model with fixed c, but will rather study the behavior of $\mathrm{Im}V_{Q\bar{Q}}$ in a class of models parametrized by c. Given that we will make c dimensionless by normalizing it at fixed temperatures and express other quantities in units of it. Moreover, it was found [37] that the range of $0\le c/T\le 2.5$ is most relevant for a comparison with QCD. We will use this range here.

On the other hand, if one works with $r=R^2/z$ as the radial coordinate, then metric (12) becomes

$$ds^2=\frac{r^2h(r)}{R^2}(-f(r)dt^2+d\vec{x}^2)+\frac{R^2h(r)}{r^2f(r)}dr^2, \tag{13}$$

with

$$f(r)=1-(1+Q^2)(\frac{r_h}{r})^4+Q^2(\frac{r_h}{r})^6,\qquad h(r)=e^{\frac{c^2R^4}{r^2}}, \tag{14}$$

now the temperature is $T=\frac{r_h}{\pi R^2}(1-\frac{Q^2}{2})$. The horizon is $r=r_h$ and the boundary is $r=\infty$. Note that (12) and (13) are equivalent but only with different coordinate systems.

3. Imaginary potential

In the holographic description [38], the heavy quark potential can be extracted from the expectation value of the static Wilson loop

$$W(C)=\frac{1}{N_c}TrPe^{i\int A_\mu dx^\mu}, \tag{15}$$

where C is a closed loop in a 4-dimensional space time and the trace is over the fundamental representation of the $SU(N_c)$ group. A_μ is the gauge potential and P enforces the path ordering along the loop C. One considers a rectangular loop with one direction along the time coordinate $\mathcal{T}$ and spatial extension L. Then the heavy quark potential, $V_{Q\bar{Q}}$, is related to the vacuum expectation of the rectangular Wilson loop in the asymptotic limit $\mathcal{T}\to\infty$,

$$<W(C)>\sim e^{-i\mathcal{T}V_{Q\bar{Q}}(L)}. \tag{16}$$

On the other hand, in the supergravity limit,

$$<W(C)>\sim e^{-iS_{str}}, \tag{17}$$

where S_{str} is the classical Nambu-Goto action of a string in the bulk,

$$S_{str}=S=-\frac{1}{2\pi\alpha'}\int d\tau d\sigma\sqrt{-det(G_{\mu\nu}\partial_aX^\mu\partial_bX^\nu)}, \tag{18}$$

where $X^\mu(\sigma,\tau)$ are worldsheet embedding coordinates with $\mu,\nu=0,1,...,4$ and $a,b=\sigma,\tau$. $\frac{1}{2\pi\alpha'}$ is the string tension and α' is related to 't Hooft coupling by $R^2/\alpha'=\sqrt{\lambda}$.

To proceed, we follow the argument in [17,18] to derive the expressions for the real and imaginary part of heavy quark potential for the background metric (13). We use the remaining symmetry of (18) to completely fix the static gauge given by

$$t=\tau,\qquad x=\sigma,\qquad y=0,\qquad z=0,\qquad r=r(\sigma). \tag{19}$$

With this gauge choice, the string action with end points fixed at $x = \pm L/2$ takes the form

$$S = \frac{\mathcal{T}}{2\pi\alpha'}\int_{-L/2}^{L/2} d\sigma \sqrt{\frac{r^4h^2(r)f(r)}{R^4} + h^2(r)(\frac{dr}{d\sigma})^2}. \tag{20}$$

Notice that the above action does not depend on σ explicitly, so the corresponding Hamiltonian is a constant

$$\mathcal{L} - \frac{\partial\mathcal{L}}{\partial(\frac{dr}{d\sigma})}\frac{dr}{d\sigma} = \frac{r^4h^2(r)f(r)/R^4}{\sqrt{\frac{r^4h^2(r)f(r)}{R^4} + h^2(r)(\frac{dr}{d\sigma})^2}} = constant. \tag{21}$$

Imposing the boundary condition at $\sigma = 0$ (the deepest point of the U-shaped string),

$$\frac{dr}{d\sigma} = 0, \qquad r = r_*, \tag{22}$$

a differential equation is derived

$$\frac{dr}{d\sigma} = \sqrt{\frac{a^2(r) - a(r)a(r_*)}{a(r_*)b(r)}}, \tag{23}$$

where

$$a(r) = \frac{r^4h^2(r)f(r)}{R^4}, \qquad a(r_*) = \frac{r_*^4h^2(r_*)f(r_*)}{R^4}, \qquad b(r) = h^2(r), \tag{24}$$

with

$$f(r_*) = 1 - (1+Q^2)(\frac{r_h}{r_*})^4 + Q^2(\frac{r_h}{r_*})^6, \qquad h(r_*) = e^{\frac{c^2R^4}{r_*^2}}. \tag{25}$$

Integrating (23), the separation length of $Q\bar{Q}$ is represented by

$$L = 2\int_{r_*}^{\infty} dr\frac{d\sigma}{dr} = 2\int_{r_*}^{\infty} dr\sqrt{\frac{a(r_*)b(r)}{a^2(r) - a(r)a(r_*)}}. \tag{26}$$

Substituting (23) into (20), the total action for $Q\bar{Q}$ reads

$$S = \frac{\mathcal{T}}{\pi\alpha'}\int_{r_*}^{\infty} dr\sqrt{\frac{a(r)b(r)}{a(r) - a(r_*)}}, \tag{27}$$

note that the above action contains the self-energy contributions from the free $Q\bar{Q}$ pair which, themselves, are divergent. To obtain the interaction potential of $Q\bar{Q}$, one needs to cure this divergence by subtracting from S the self energy of the two quarks [38–40]. As a result, the real part of the heavy quark potential in the $SW_{T,\mu}$ model is

$$ReV_{Q\bar{Q}} = \frac{1}{\pi\alpha'}\int_{r_*}^{\infty} dr[\sqrt{\frac{a(r)b(r)}{a(r) - a(r_*)}} - \sqrt{b_0(r)}] - \frac{1}{\pi\alpha'}\int_{r_h}^{r_*}\sqrt{b_0(r)}dr, \tag{28}$$

with $b_0(r) = b(r \to \infty)$. Here we would like to discuss our expectations for the heavy quark potential on the field theory side. For small distance L, one expects the thermodynamic variables T and μ, as well as a possible confining (or deformation) scale c, to have negligible effect on the interaction potential of $Q\bar{Q}$. This argument is backed by lattice results [41,42] which show that for $LT << 1$ the free energy is independent of T. Moreover, if $Q\bar{Q}$ interaction does not depend for small L on T, μ and c, the regularization in (28) does not depend on these scales either.

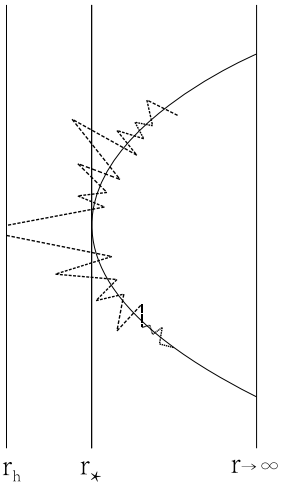

Fig. 1. The effect of thermal fluctuations (dashed line) around the classical configuration (solid line). If r_* is close enough to r_h, the fluctuations of very long wavelength may reach the horizon.

Next, we derive the expressions of $\mathrm{Im}V_{Q\bar{Q}}$ using the string worldsheet fluctuations [17,18]. Considering the effect of thermal world sheet fluctuations $\delta r(x)$ around the classical configurations $r_c(x)$,

$$r(x) = r_c(x) \to r(x) = r_c(x) + \delta r(x), \tag{29}$$

where $r_c(x)$ solves $\delta S_{NG} = 0$, and the boundary condition is $\delta r(\pm L/2) = 0$. For simplicity, $\delta r(x)$ is taken to be of arbitrarily long wavelength, i.e., $\frac{d\delta r(x)}{dx} \to 0$. So the fluctuations at each string point are independent functions if one considers the long wavelength limit. The physical picture of the thermal fluctuations is illustrated in Fig. 1.

The string partition function that takes into account the fluctuations is

$$Z_{str} \sim \int \mathcal{D}\delta r(x) e^{iS_{NG}(r_c(x)+\delta r(x))}. \tag{30}$$

Dividing the interval $-L/2 < x < L/2$ into $2N$ points $x_j = j\Delta x$ with $j = -N, -N+1, ..., N$ and $\Delta x \equiv L/(2N)$, one gets

$$Z_{str} \sim \lim_{N\to\infty}\int d[\delta r(x_{-N})]\cdots d[\delta r(x_N)] \times exp[\frac{i\mathcal{T}\Delta x}{2\pi\alpha'}\sum_j\sqrt{b(r_j)(r_j')^2 + a(r_j)}], \tag{31}$$

with $r_j \equiv r(x_j)$ and $r_j' \equiv r'(x_j)$. The thermal fluctuations are more important around $x = 0$, where $r = r_*$. Thus, it is reasonable to expand $r_c(x_j)$ around $x = 0$, keeping only terms up to second order in x_j. As $r_c'(0) = 0$, one has

$$r_c(x_j) \approx r_* + \frac{x_j^2}{2}r_c''(0). \tag{32}$$

On the other hand, the expansion for $a(r_j)$, keeping only terms up to second order in $x_j^m\delta r_n$, takes the form

$$a(r_j) \approx a_* + \delta r a_*' + r_c''(0)a_*'\frac{x_j^2}{2} + \frac{\delta r^2}{2}a_*'', \tag{33}$$

with $a_* \equiv a(r_*)$, $a'_* \equiv a'(r_*)$, etc. As a result, the exponent in (31) can be written as

$$S_j^{NG} = \frac{\mathcal{T}\Delta x}{2\pi\alpha'}\sqrt{C_1 x_j^2 + C_2}, \tag{34}$$

with

$$C_1 = \frac{r_c''(0)}{2}[2b_* r_c''(0) + a'_*], \qquad C_2 = a_* + \delta r a'_* + \frac{\delta r^2}{2}a''_*, \tag{35}$$

where $b_* \equiv b(r_*)$.

If the function in the square root of (34) is negative, S_j^{NG} will contribute to $\mathrm{Im}V_{Q\,Q} \neq 0$. The relevant region of the fluctuations is the one between δr that yields a vanishing argument in the square root of (34). Therefore, one can isolate the j-th contribution as

$$I_j \equiv \int_{\delta r_{jmin}}^{\delta r_{jmax}} d(\delta r_j) exp[\frac{i\mathcal{T}\Delta x}{2\pi\alpha'}\sqrt{C_1 x_j^2 + C_2}], \tag{36}$$

where δr_{jmin} and δr_{jmax} are the roots of $C_1 x_j^2 + C_2$ in δr.

The integral in (36) can be determined by using the saddle point method for $\alpha' << 1$ (the classical gravity approximation). The exponent has a stationary point when the function inside the root square of (36)

$$D(\delta r_j) \equiv C_1 x_j^2 + C_2(\delta r_j), \tag{37}$$

assumes an extremal value. This happens for

$$\delta r = -\frac{a'_*}{a''_*}. \tag{38}$$

It is required that the square root has an imaginary part, yielding

$$D(\delta r_j) < 0 \rightarrow -x_c < x_j < x_c, \tag{39}$$

with

$$x_c = \sqrt{\frac{1}{C_1}(\frac{a'^2_*}{2a''_*} - a_*)}. \tag{40}$$

Taking $x_c = 0$ if the square root in (40) is not real. With these conditions, one can approximate $D(\delta r)$ by $D(-\frac{a'_*}{a''_*})$ in (36)

$$I_j \sim exp[\frac{i\mathcal{T}\Delta x}{2\pi\alpha'}\sqrt{C_1 x_j^2 + a_* - \frac{a'^2_*}{2a''_*}}]. \tag{41}$$

The total contribution to the imaginary part comes from $\Pi_j I_j$, yielding

$$ImV_{Q\,\bar{Q}} = -\frac{1}{2\pi\alpha'}\int_{|x|<x_c} dx\sqrt{-x^2 C_1 - a_* + \frac{a'^2_*}{2a''_*}}. \tag{42}$$

Integrating (42), one ends up with the imaginary potential in the $SW_{T,\mu}$ model

$$ImV_{Q\,\bar{Q}} = -\frac{1}{2\sqrt{2}\alpha'}\sqrt{b_*}(\frac{a'_*}{2a''_*} - \frac{a_*}{a'_*}), \tag{43}$$

with

$$\begin{aligned}
a'_* &= 2r_*^4 h(r_*)h'(r_*)f(r_*) + r_*^4 h^2(r_*)f'(r_*) + 4r_*^3 h^2(r_*)f(r_*),\\
a''_* &= 2r_*^4 h(r_*)h''(r_*)f(r_*) + r_*^4 h^2(r_*)f''(r_*)\\
&\quad + 16r_*^3 h(r_*)h'(r_*)f(r_*) + 8r_*^3 h^2(r_*)f'(r_*)\\
&\quad + 4r_*^4 h(r_*)h'(r_*)f'(r_*) + 2r_*^4 h'(r_*)h'(r_*)f(r_*)\\
&\quad + 12r_*^2 h^2(r_*)f(r_*),\\
f'(r_*) &= 4(1 + \frac{\mu^2}{3r_h^2})r_h^4 r_*^{-5} - 2\mu^2 r_h^4 r_*^{-7},\\
f''(r_*) &= -20(1 + \frac{\mu^2}{3r_h^2})r_h^4 r_*^{-6} + 14\mu^2 r_h^4 r_*^{-8},\\
h'(r_*) &= -2c^2 r_*^{-3} e^{\frac{c^2}{r_*^2}}, \qquad h''(r_*) = (6c^2 r_*^{-4} + 4c^4 r_*^{-6})e^{\frac{c^2}{r_*^2}},
\end{aligned} \tag{44}$$

where, for convenience, we have set $R = 1GeV^{-1}$. Notice that the $\mathrm{Im}V_{Q\,\bar{Q}}$ of $\mathcal{N} = 4$ SYM plasma [17] can be derived from (43) if one neglects the effect of chemical potential and confining scale by plugging $\mu = c = 0$ in (43).

4. Numerical results

Before going further, we discuss the regime of applicability of this model. First, $\mathrm{Im}V_{Q\,\bar{Q}}$ should be negative, implying

$$\frac{a'_*}{2a''_*} - \frac{a_*}{a'_*} > 0, \tag{45}$$

which leads to

$$\varepsilon > \varepsilon_{min}, \tag{46}$$

with $\varepsilon = r_h/r_*$, where the value of ε_{min} can be determined numerically.

The second limitation relates to LT_{max}, the maximum value of LT. From (10), (11) and (26), one gets

$$LT = (\frac{2r_h}{\pi} - \frac{\mu^2}{3\pi r_h})\int_{r_*}^{\infty} dr\sqrt{\frac{a(r_*)b(r)}{a^2(r) - a(r)a(r_*)}}. \tag{47}$$

In Fig. 2, we plot LT as a function of ε for various cases. One can see that there exists a LT_{max} (corresponds to $\varepsilon = \varepsilon_{max}$) in each plot. As discussed in [20], LT_{max} indicates the limit of the saddle point approximation: for $\varepsilon > \varepsilon_{max}$, there are other string configurations (which are not solutions of the Nambu-Goto action) that may contribute to the calculation of the Wilson loops besides the semi-classical U-shaped string configuration [43]. Here we focus mainly on the case where $\varepsilon < \varepsilon_{max}$. Taken together, the domain of applicability of (43) is $\varepsilon_{min} < \varepsilon < \varepsilon_{max}$.

To proceed, we investigate the effect c and μ on the inter-distance. From the left (or right) panel of Fig. 2, one can see that at fixed c, increasing μ leads to decreasing LT. On the other hand, by comparing the left panel with the right one, one finds that at fixed μ, increasing c leads to increasing LT. Therefore, one concludes that the chemical potential reduces the inter-distance while the confining scale enhances it.

Next, we study how c and μ influence the imaginary potential. For this purpose, in Fig. 3 we plot $\mathrm{Im}V/(\sqrt{\lambda}T)$ versus LT for various cases. One sees that in each plot the imaginary potential starts at a LT_{min}, corresponding to ε_{min} (or $\mathrm{Im}V_{Q\,\bar{Q}} = 0$), and ends at a LT_{max}, corresponding to ε_{max}. Moreover, from the left (or right) panel, one finds that at fixed c, for increasing μ the onset of the imaginary potential occurs at smaller values of LT, consistently with the findings of [22]. Also, by comparing the left panel with

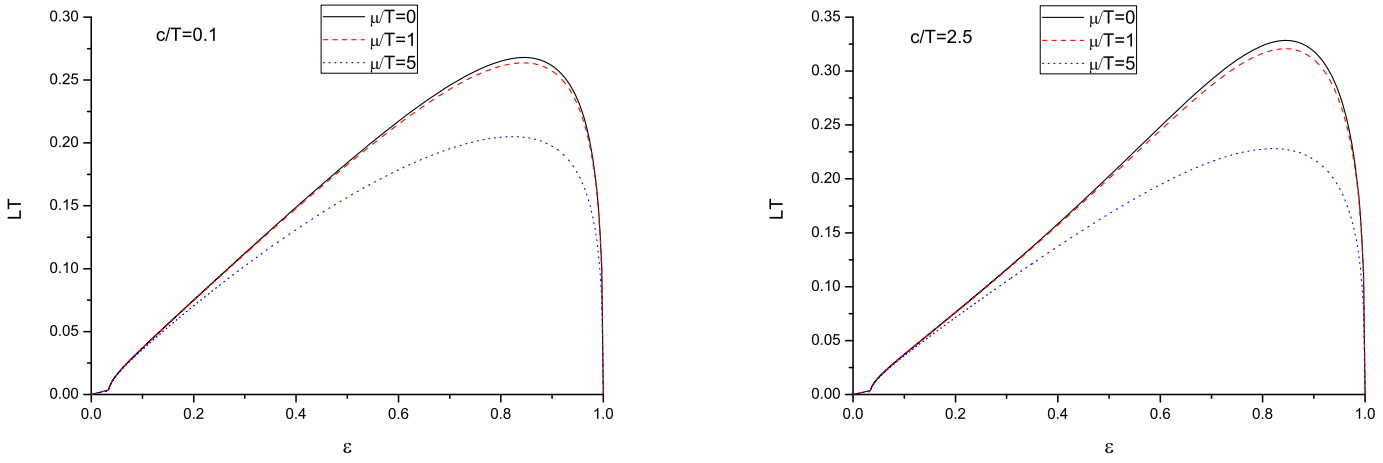

Fig. 2. LT versus ε. Left: $c/T = 0.1$. Right: $c/T = 2.5$. In both panels from top to bottom, $\mu/T = 0, 1, 5$, respectively.

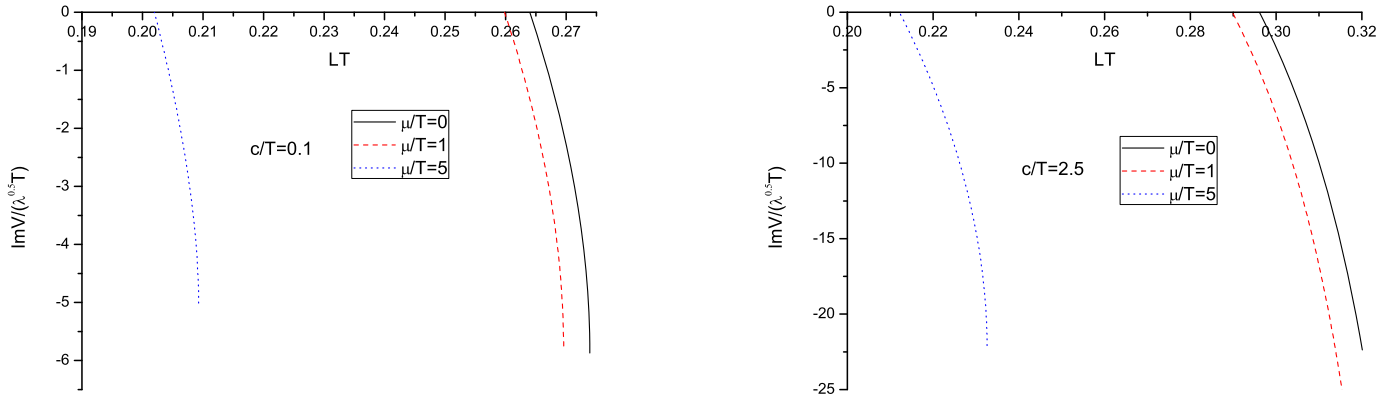

Fig. 3. $\mathrm{Im}V/(\sqrt{\lambda}T)$ versus LT. Left: $c/T = 0.1$. Right: $c/T = 2.5$. In both panels from right to left, $\mu/T = 0, 1, 5$, respectively.

the right one, one can see that at fixed μ, increasing c the imaginary potential happens for larger values of LT, in accordance with [25]. As discussed in [20], the dissociation properties of quarkonia is sensitive to the imaginary potential, and if the onset of the imaginary potential happens for smaller LT, the suppression will be stronger. Consequently, one concludes that the inclusion of the chemical potential makes quarkonia dissociation easier, while the confining scale makes it harder.

Also, one could analyze how c and μ affect the thermal width. As we known, the imaginary potential can be used to estimate the thermal width and usually a larger absolute value of imaginary potential corresponds to larger thermal width [17,18]. Thus, one could say that the presence of a chemical potential decreases the thermal width while the confining scale increases it.

Finally, since c and μ have opposite effects on the imaginary potential, one can infer that with some chosen values of c and μ, the $\mathrm{Im}V_{Q\bar{Q}}$ can be larger or smaller than its counterpart of $\mathcal{N} = 4$ SYM theory. In other words, this model provides a wider range of values for the $\mathrm{Im}V_{Q\bar{Q}}$ in comparison to that found in $\mathcal{N} = 4$ SYM case.

5. Conclusion and discussion

In this paper, we studied the $\mathrm{Im}V_{Q\bar{Q}}$ of a heavy quarkonium at finite temperature and chemical potential in a holographic AdS/QCD model with conformal invariance broken by a background dilaton. We discussed the effects of deformation parameter c and chemical potential μ on this quantity, respectively. It is found that c and μ have opposing effects on $\mathrm{Im}V_{Q\bar{Q}}$. Specifically, the presence of c increases the absolute value of $\mathrm{Im}V_{Q\bar{Q}}$ while μ decreases it. One step further, the inclusion of the confining scale makes dissociation harder while the chemical potential makes it easier, which confirms earlier findings. In addition, it is shown that this model provides a wider range of values for the $\mathrm{Im}V_{Q\bar{Q}}$ in comparison to that found in $\mathcal{N} = 4$ SYM theory.

However, it should be admitted that the $\mathrm{SW}_{T,\mu}$ model considered here is not consistent model since it does not solve the full set of equations of motion associated with action (1). Rather, it could be regarded as a crude approximation in which one solves the Einstein-Maxwell part of the action, and then the scalar part with the background metric. Despite this, one can take advantage of its simplicity (e.g., the horizon function remains relatively simple) and get some useful information [30–34]. Certainly, it would be significant to study the $\mathrm{Im}V_{Q\bar{Q}}$ in some consistent models, e.g. [44–46] and compare the results obtained in those models and ours (but usually the metrics of those models are only known numerically, so it would technically be rather challenging). Also, it is of interest to see what happens in holographic models that aim at realistically describing the properties of the QGP in equilibrium at finite temperature and density, which also include a realistic prediction for the QCD critical point, e.g. [47]. We plan to come back to these issues in future work.

Acknowledgements

We would like to thank the anonymous referee for his/her valuable comments and helpful advice. This work is supported by the

NSFC under Grant No. 11705166 and the Fundamental Research Funds for the Central Universities, China University of Geosciences (Wuhan) (No. CUGL180402). The work of Xiangrong Zhu is supported by Zhejiang Provincial Natural Science Foundation of China No. LY19A050001.

References

[1] E.V. Shuryak, Phys. Rep. 61 (1980) 71.
[2] F. Karsch, M.T. Mehr, H. Satz, Z. Phys. C 37 (1988) 617.
[3] M. Laine, O. Philipsen, P. Romatschke, M. Tassler, J. High Energy Phys. 03 (2007) 054.
[4] A. Beraudo, J.-P. Blaizot, C. Ratti, Nucl. Phys. A 806 (2008) 312.
[5] N. Brambilla, J. Ghiglieri, A. Vairo, P. Petreczky, Phys. Rev. D 78 (2008) 014017.
[6] M.A. Escobedo, J. Phys. Conf. Ser. 503 (2014) 012026.
[7] Y. Burnier, M. Laine, M. Vepsäläinen, Phys. Lett. B 678 (2009) 86.
[8] A. Dumitru, Y. Guo, M. Strickland, Phys. Rev. D 79 (2009) 114003.
[9] N. Brambilla, M.A. Escobedo, J. Ghiglieri, J. Soto, A. Vairo, J. High Energy Phys. 09 (2010) 038.
[10] M. Margotta, K. McCarty, C. McGahan, M. Strickland, D.Y. Elorriaga, Phys. Rev. D 83 (2011) 105019.
[11] V. Chandra, V. Ravishankar, Nucl. Phys. A 848 (2010) 330.
[12] U.W. Heinz, R. Snellings, Annu. Rev. Nucl. Part. Sci. 63 (2013) 123–151.
[13] J.M. Maldacena, Adv. Theor. Math. Phys. 2 (1998) 231.
[14] S.S. Gubser, I.R. Klebanov, A.M. Polyakov, Phys. Lett. B 428 (1998) 105.
[15] O. Aharony, S.S. Gubser, J. Maldacena, H. Ooguri, Y. Oz, Phys. Rep. 323 (2000) 183.
[16] J.C. Solana, H. Liu, D. Mateos, K. Rajagopal, U.A. Wiedemann, arXiv:1101.0618.
[17] J. Noronha, A. Dumitru, Phys. Rev. Lett. 103 (2009) 152304.
[18] S.I. Finazzo, J. Noronha, J. High Energy Phys. 11 (2013) 042.
[19] K.B. Fadafan, D. Giataganas, H. Soltanpanahi, J. High Energy Phys. 11 (2013) 107.
[20] S.I. Finazzo, J. Noronha, J. High Energy Phys. 01 (2015) 051.
[21] M. Ali-Akbari, D. Giataganas, Z. Rezaei, Phys. Rev. D 90 (2014) 086001.
[22] Z.q. Zhang, D.f. Hou, G. Chen, Phys. Lett. B 768 (2017) 180.
[23] K.B. Fadafan, S.K. Tabatabaei, J. Phys. G, Nucl. Part. Phys. 43 (2016) 095001.
[24] N.F. Braga, L.F. Ferreira, Phys. Rev. D 94 (2016) 094019.
[25] J. Sadeghi, S. Tahery, J. High Energy Phys. 06 (2015) 204.
[26] J.L. Albacete, Y.V. Kovchegov, A. Taliotis, Phys. Rev. D 78 (2008) 115007.
[27] T. Faulkner, H. Liu, Phys. Lett. B 673 (2009) 161.
[28] T. Hayata, K. Nawa, T. Hatsuda, Phys. Rev. D 87 (2013) 101901(R).
[29] A. Karch, E. Katz, D.T. Son, M.A. Stephanov, Phys. Rev. D 74 (2006) 015005.
[30] P. Colangelo, F. Giannuzzi, S. Nicotri, Phys. Rev. D 83 (2011) 035015.
[31] C. Park, D.-Y. Gwak, B.-H. Lee, Y. Ko, S. Shin, Phys. Rev. D 84 (2011) 046007.
[32] P. Colangelo, F. Giannuzzi, S. Nicotri, J. High Energy Phys. 1205 (2012) 076.
[33] P. Colangelo, F. Giannuzzi, S. Nicotri, F. Zuo, Phys. Rev. D 88 (2013) 115011.
[34] X. Chen, S.-Q. Feng, Y.-F. Shi, Y. Zhong, Phys. Rev. D 97 (2018) 066015.
[35] O. DeWolfe, S.S. Gubser, C. Rosen, Phys. Rev. D 83 (2011) 086005.
[36] O. Andreev, V.I. Zakharov, Phys. Lett. B 645 (2007) 437.
[37] H. Liu, K. Rajagopal, Y. Shi, J. High Energy Phys. 0808 (2008) 048.
[38] J.M. Maldacena, Phys. Rev. Lett. 80 (1998) 4859.
[39] S.-J. Rey, S. Theisen, J.-T. Yee, Nucl. Phys. B 527 (1998) 171.
[40] A. Brandhuber, N. Itzhaki, J. Sonnenschein, S. Yankielowicz, Phys. Lett. B 434 (1998) 36.
[41] O. Kaczmarek, F. Karsch, F. Zantow, P. Petreczky, Phys. Rev. D 70 (2004) 074505.
[42] O. Kaczmarek, F. Zantow, Phys. Rev. D 71 (2005) 114510.
[43] D. Bak, A. Karch, L.G. Yaffe, J. High Energy Phys. 0708 (2007) 049.
[44] A. Stoffers, I. Zahed, Phys. Rev. D 83 (2011) 055016.
[45] S. He, S.-Y. Wu, Y. Yang, P.-H. Yuan, J. High Energy Phys. 1304 (2013) 093.
[46] R. Rougemont, A. Ficnar, S. Finazzo, J. Noronha, J. High Energy Phys. 04 (2016) 102.
[47] R. Critelli, J. Noronha, J.N. Hostler, I. Portillo, C. Ratti, R. Rougemont, Phys. Rev. D 96 (2017) 096026.